Mon. Not. R. Astron. Soc. **311**, 370–376 (2000)

Ultra-high-resolution observations of circumstellar K I and C_2 around the post-AGB star HD 56126

I. A. Crawford and M. J. Barlow

Department of Physics and Astronomy, University College London, Gower Street, London WC1E 6BT

Accepted 1999 August 17. Received 1999 July 26; in original form 1999 May 14

ABSTRACT

We have used the Ultra-High-Resolution Facility (UHRF) at the AAT, operating at a resolution of $0.35\,\mathrm{km\,s^{-1}}$ (FWHM), to observe K I and C_2 absorption lines arising in the circumstellar environment of the post-AGB star HD 56126. We find three narrow circumstellar absorption components in K I, two of which are also present in C_2. We attribute this velocity structure to discrete shells resulting from multiple mass-loss events from the star. The very high spectral resolution has enabled us to resolve the intrinsic linewidths of these narrow lines for the first time, and we obtain velocity dispersions (b-values) of 0.2–0.3 $\mathrm{km\,s^{-1}}$ for the K I components, and $0.54 \pm 0.03\,\mathrm{km\,s^{-1}}$ for the strongest (and best defined) C_2 component. These correspond to rigorous kinetic temperature upper limits of 211 K for K I and 420 K for C_2, although the b-value ratio implies that these two species do not co-exist spatially. The observed degree of rotational excitation of C_2 implies low kinetic temperatures ($T_k \approx 10$ K) and high densities ($n \approx 10^6$ to $10^7\,\mathrm{cm^{-3}}$) within the shell responsible for the main C_2 component. Given this low temperature, the line profiles then imply either mildly supersonic turbulence or an unresolved velocity gradient through the shell.

Key words: molecular processes – stars: AGB and post-AGB – circumstellar matter – stars: individual: HD 56126.

1 INTRODUCTION

Asymptotic giant branch (AGB) stars enrich the interstellar medium, and thus future generations of stars, in the products of stellar nucleosynthesis, particularly carbon and the s-process elements. This material is expelled into the interstellar medium via powerful stellar winds. During the relatively fast evolution across the Hertzsprung–Russell (HR) diagram following departure from the AGB and before the central star becomes hot enough to illuminate the ejecta as an ionized planetary nebula, the optical spectra of post-AGB objects can mimic those of A–K-type supergiants. The true nature of many of these sources was only recognized when the *IRAS* survey detected strong circumstellar dust emission that originated from their optically invisible ejected envelopes.

The carbon-rich nature of many of these objects was confirmed by Hrivnak (1995) who reported C_2 and C_3 absorption bands in the spectra of nine supergiant-spectrum post-AGB sources, observed at medium (~3 Å) resolution. These stars had previously been identified by Kwok et al. (Kwok, Volk & Hrivnak 1989; Kwok, Hrivnak & Geballe 1995) and Hrivnak & Kwok (1991) as carriers of a very strong unidentified emission feature at 21 μm. Recently, Bakker (1995) and Bakker et al. (1996, 1997) detected narrow circumstellar absorption lines of C_2 and CN in the spectra of 11 of these objects, and showed that these lines are not photospheric but arise from detached expanding circumstellar shells around the stars. These molecules are presumed to form in dense shells arising from the last phase of AGB mass loss.

The physical conditions (temperature, density and turbulence) of this material are of interest because of what they tell us about the final stages of stellar evolution. In principle, the profiles of absorption lines arising in the circumstellar shell can be used to derive information concerning these conditions, although the lines are so narrow that very high spectral resolution is required. The observations of Bakker et al. employed a resolving power of $R \equiv \lambda/\Delta\lambda \approx 50\,000$ ($6\,\mathrm{km\,s^{-1}}$ FWHM), which was insufficient to resolve the intrinsic line proliles. Here we report observations of circumstellar K I and C_2 lines towards the eighth-magnitude ($V = 8.23$) post-AGB F5I star HD 56126 (IRAS 07134+1005), obtained at $R \approx 900\,000$, over an order of magnitude higher than that employed by Bakker (1995) and Bakker et al. (1996, 1997). This very high spectral resolution has now enabled us to resolve the intrinsic line profiles, and to place tighter constraints on the physical conditions prevailing in the circumstellar environment.

2 OBSERVATIONS

The observations reported here were obtained with the Ultra-High-Resolution Facility (UHRF) at the Anglo-Australian Telescope over three nights (1999 January 28–30, inclusive). A total of four

1200-s integrations were obtained of the region containing the K I resonance line at 7699 Å, and 11 1200-s integrations (through varying amounts of cloud) of a region containing part of the C_2 (2–0) Phillips band near 8760 Å. The detector was the AAO MIT/LL2 CCD (4096 × 2048 15-μm pixels), which resulted in a wavelength coverage of 12.1 Å for the latter observations, allowing us to detect six lines within the C_2 band for a single wavelength setting. All the lines observed, together with their rest wavelengths and adopted oscillator strengths, are listed in Table 1.

The spectrograph was operated with a confocal image slicer (Diego 1993), and the CCD output was binned by a factor of eight perpendicular to the dispersion direction in order to reduce the readout noise associated with extracting the broad spectrum produced by the image slicer. The velocity resolution, measured from the observed width of a stabilized He–Ne laser line, was $0.35 \pm 0.01\,\mathrm{km\,s^{-1}}$ (FWHM), corresponding to a resolving power of $R = 860\,000$. Other aspects of the instrument and observing procedures have been described in detail by Diego et al. (1995) and Barlow et al. (1995).

The spectra were extracted from the individual CCD images using the FIGARO data-reduction package (Shortridge 1988) at the UCL Starlink node. Scattered light and CCD dark current were measured from the inter-order region and subtracted (see below), and the spectra were divided by a flat-field. Wavelength calibration was performed using a Th–Ar lamp; second order fits to the five (K I region) and four (C_2 region) Th–Ar lines identified in these wavelength ranges yielded rms residuals of $\lesssim 1 \times 10^{-3}$ Å (or $\lesssim 0.03\,\mathrm{km\,s^{-1}}$) in both cases. Once wavelength calibrated, the spectra were converted to the heliocentric velocity frame (adopting rest wavelengths given in Table 1), and the individual exposures were added. The entire spectrum of the C_2 region is shown in Fig. 1, while a close-up of the K I region is shown in Fig. 2.

It is immediately apparent from Fig. 1 that the noise in the final

Table 1. Circumstellar lines observed in the present study. Wavelengths (λ) and oscillator stengths (f) are from Morton (1991) for K I and Bakker (1995) for C_2; W_λ is the total equivalent width (i.e. summed over all velocity components), while ΔW_λ gives the percentage difference between the values obtained here and those obtained by Bakker (1995); $v_{\rm helio}$, b and N are the heliocentric velocities, velocity dispersions, and column densities of the model line profiles shown in Figs 2 and 3. Powers of 10 are given in parentheses.

Line	λ (Å)	f	W_λ(here) (mÅ)	W_λ(Bakker) (mÅ)	ΔW_λ	$v_{\rm helio}$ ($\mathrm{km\,s^{-1}}$)	b ($\mathrm{km\,s^{-1}}$)	N ($\mathrm{cm^{-2}}$)
K I	7698.974	3.39(−1)	45.0 ± 2.5	…	…	75.50 ± 0.08	0.30 ± 0.05	$1.00^{+0.10}_{-0.20}$ (11)
						76.52 ± 0.05	0.20 ± 0.05	$1.90^{+0.30}_{-0.10}$ (11)
						77.56 ± 0.04	0.20 ± 0.05	$2.70^{+0.10}_{-0.70}$ (11)
C_2 R(0)	8757.686	1.67(−3)	37.4 ± 1.6	33.2	+13%	76.67 ± 0.23	0.60 ± 0.10	5.0 ± 2.0 (12)
						77.77 ± 0.03	0.55 ± 0.10	5.0 ± 1.0 (13)
C_2 Q(2)	8761.194	8.35(−4)	45.0 ± 1.5	42.5	+6%	76.50 ± 0.07	0.60 ± 0.10	2.7 ± 0.4 (13)
						77.66 ± 0.03	0.50 ± 0.05	1.2 ± 0.2 (14)
C_2 P(2)	8766.031	1.67(−4)	27.0 ± 1.2	22.9	+18%	76.66*		< 2.0 (13)
						77.76 ± 0.02	0.55 ± 0.10	3.5 ± 0.5 (14)
C_2 Q(4)	8763.754	8.35(−4)	47.0 ± 1.4	50.0	−6%	76.18 ± 0.09	0.60 ± 0.10	2.3 ± 0.4 (13)
						77.35 ± 0.03	0.55 ± 0.05	1.5 ± 0.2 (14)
C_2 R(12)	8757.130	4.68(−4)	26.0 ± 1.4	32.0	−19%	76.65*	0.60 ± 0.10	8.0 ± 3.0 (12)
						77.75 ± 0.03	0.55 ± 0.05	1.1 ± 0.3 (14)
C_2 R(14)	8762.147	4.61(−4)	22.0 ± 1.2	25.6	−14%	76.53*		< 5.0 (12)
						77.63 ± 0.03	0.60 ± 0.10	1.1 ± 0.3 (14)

* The velocity splittings of these weak C_2 components relative to the main component have been fixed to be $1.1\,\mathrm{km\,s^{-1}}$; i.e. the velocity separation determined for the stronger lines.

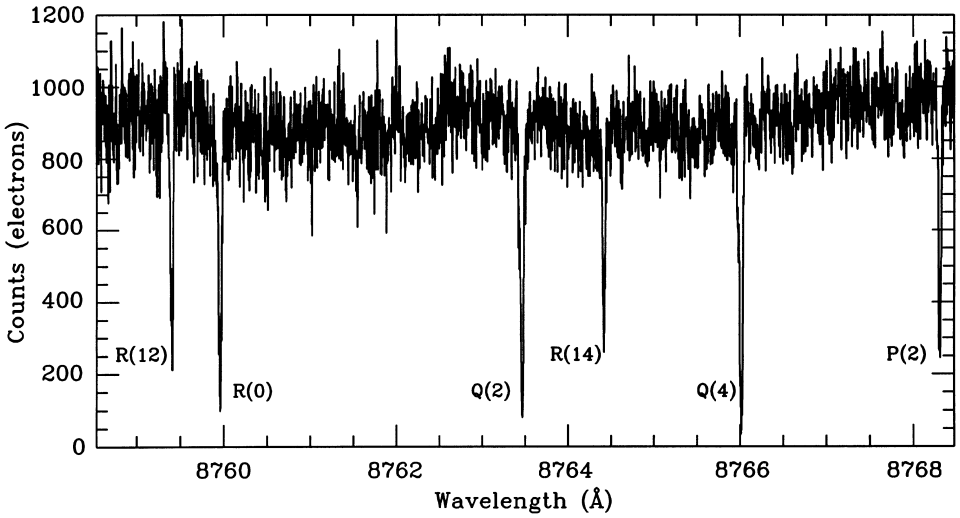

Figure 1. The circumstellar C_2 lines observed towards HD 56126.

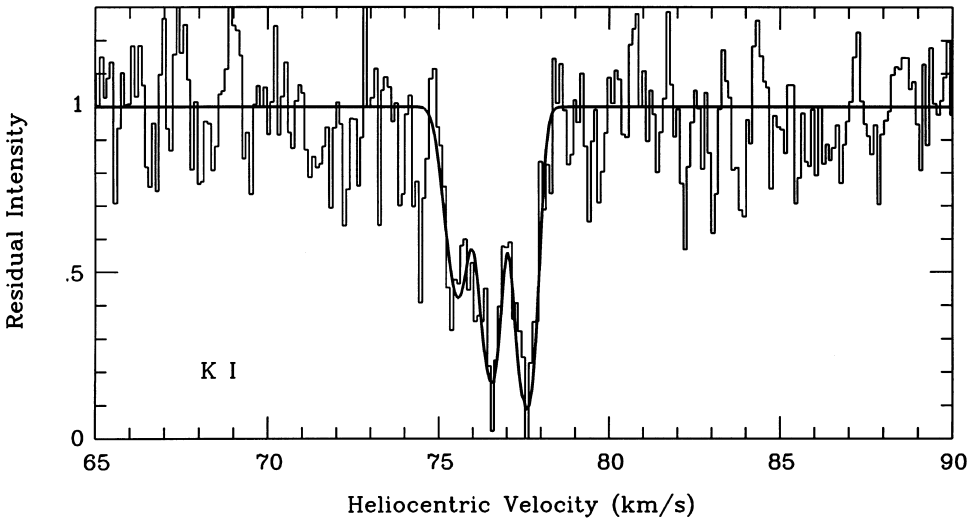

Figure 2. The circumstellar K I 7699 Å line observed towards HD 56126.

spectrum (≈9.5 per cent rms) is about three times worse than would be implied by photon statistics given the number of continuum counts obtained. This is owing to high backgrounds in the raw data, resulting from a combination of high detector dark current and a known problem of low-level fluorescence from the AAT coude room walls. As regards the dark current, we measured an average value of 0.72 electron pixel^{-1} h^{-1} (which is a factor of 2.7 times higher than expected from measurements provided by the observatory), and which gives a background contribution of approximately 630 electron h^{-1} per extracted pixel in the final spectrum (extracted over approximately 110 binned CCD pixels). This is sufficient to dominate the total number of counts obtained for this (by UHRF standards) very faint object.

These high backgrounds may cast some doubt on the photometric accuracy of the present observations, and therefore on the derived equivalent widths and column densities. For this reason, Table 1 compares our equivalent widths with those obtained previously by Bakker (1995), and it will be seen that the two sets of data agree to within 10–20 per cent. Moreover, it is clear that there is no *systematic* discrepancy between these results: Table 1 (column 6) shows that for half of the C_2 lines observed our equivalent widths are larger than those obtained by Bakker et al., while for the other half they are smaller, and that the differences do not show any trend with wavelength. Finally, we note that our adopted background level cannot underestimate the true value by more than 10 per cent (90 counts) without causing the cores of the strongest lines to fall below zero residual intensity. For these reasons, we feel that, in spite of the high backgrounds, our continuum level is accurate to within about 10 per cent. We note that while a 10 per cent uncertainty in the continuum level will result in a significant uncertaintly in the column densities derived for these quite saturated lines, it has a negligible influence on the derived line *widths* which are the primary results of the present paper.

The circumstellar lines were modelled using the interstellar-line-fitting routines in the DIPSO spectral analysis program (Howarth, Murray & Mills 1993). The best-fitting Voigt profiles, after convolution with the instrumental response function, are also shown in Fig. 2 for the K I line and Fig. 3 for the six C_2 lines. The resulting line profile parameters (heliocentric velocity, $v_{\rm helio}$, velocity dispersion, b, and column density, N) are listed in Table 1. Note that the theoretical K I line profiles include the effect of hyperfine splitting: this amounts to 0.35 km s^{-1} for this atom (e.g. Welty, Hobbs & Kulkarni 1994), and although it has not been resolved it neverthelsss broadens the line profiles significantly.

3 DISCUSSION

3.1 K I

As noted by Bakker (1995) and Bakker et al. (1996), strong absorption lines from resonance atomic transitions are expected to arise in the cool circumstellar shells of post-AGB stars, and they presented observations of circumstellar Na D lines for HD 56126. These authors found complicated Na D line profiles with six discrete absorption components apparent at their resolution, most of which they attribute to interstellar absorption. However, they identified a strong component at $v_{\rm helio} = 75 \pm 3$ km s^{-1} as circumstellar, as it occurs at the same radial velocity as the molecular lines.

We expect absorption components observed in Na I to be also present in K I, owing to the similar ionization potentials of these atoms. Moreover, we note that resonantly scattered circumstellar K I emission has been previously detected from mass-losing stars (e.g. from the M supergiants α Ori and μ Cep, Mauron & Querci 1990; or from N-type carbon stars, Gustafsson et al. 1997), so we expect circumstellar K I to be present towards HD 56126. Fig. 2 shows this expectation to be confirmed, with the clear detection of a strong, and apparently multiple, K I absorption feature occupying the velocity range expected for the circumstellar material.

For the reasons given in Section 2, the signal-to-noise ratio is poor, and this may cast some doubt on the statistical significance of the claimed multiple velocity structure. This would then imply that the data are consistent with a single, broad, approximately trapezoidal-shaped absorption line, such as might be expected from a continuous outflow. However, the fact that the two strongest 'features' within the core of the broad K I absorption occur at essentially the same velocities as the discrete components observed in the higher signal-to-noise C_2 data (see below), supports the view that multiple K I velocity components are present. For this reason, we favour the three-component fit shown in Fig. 2, with the parameters listed in Table 1.

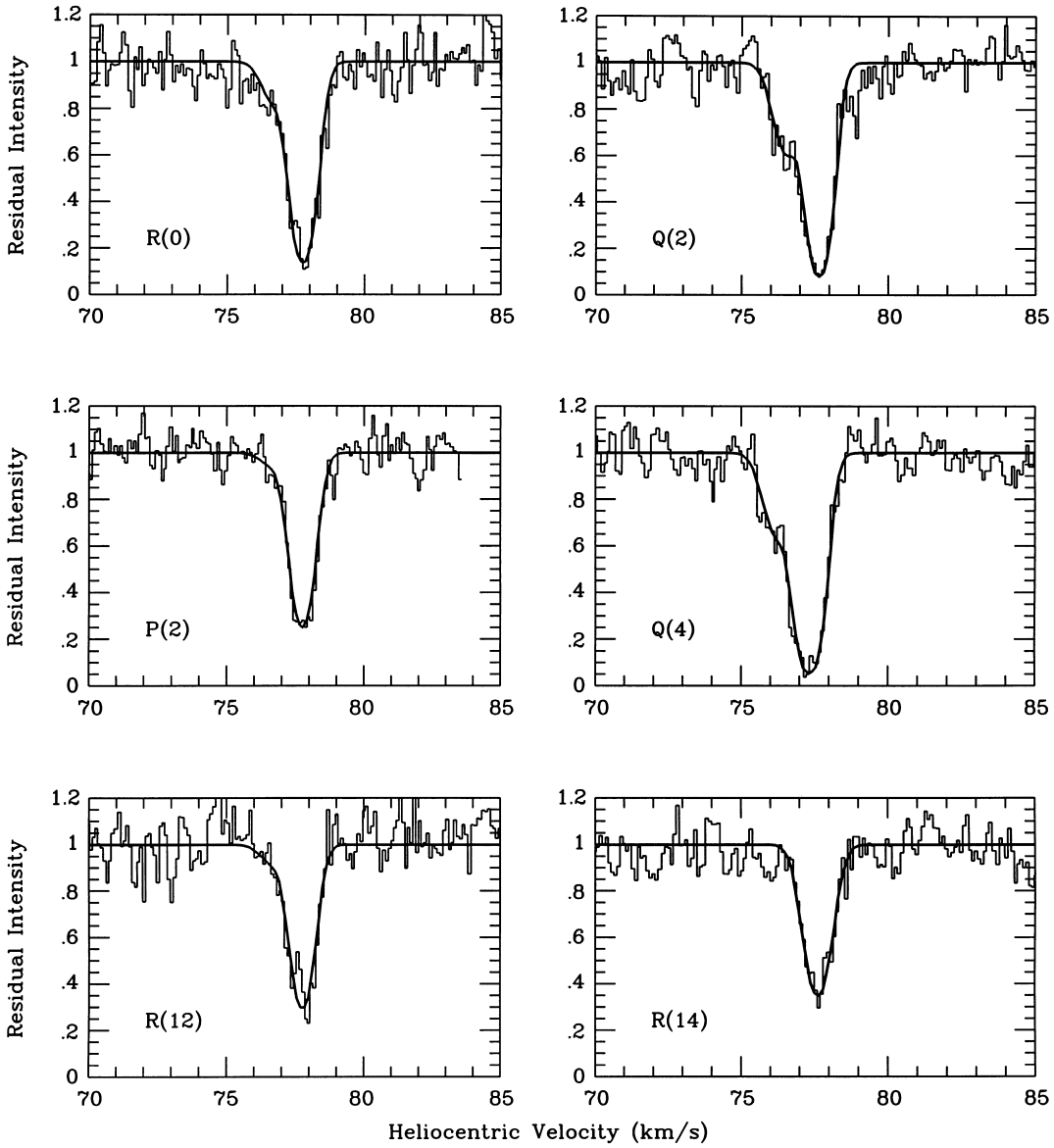

Figure 3. The individual circumstellar C_2 lines observed towards HD 56126. The observed data are plotted as histograms. The smooth curves are theoretical line profiles with the parameters listed in Table 1.

We interpret these components as being associated with three distinct shells. We note that there appears to be a trend with radial velocity, in the sense that that the most blueshifted K I component has no obvious C_2 counterpart (see Section 3.2 below), the central K I component is weak in C_2, and the least blueshifted K I component is the strongest in C_2. By themselves, the radial velocities do not provide a model-independent means of determining the relative locations of the different shells. However, it seems likely that the least blueshifted component is the most recently ejected (and hence closest to the star) simply on the grounds that it would be expected to have the highest density, favouring the formation and shielding of molecules such as C_2.

The integrated CO $J = 2 - 1$ emission from the entire circumstellar envelope of HD 56126, observed by Knapp et al. (1998) with a velocity resolution of $0.12\,\mathrm{km\,s^{-1}}$, does not show evidence for discrete components in its overall parabolic profile. Relative to the stellar (heliocentric) central velocity of $+87.5 \pm 0.8\,\mathrm{km\,s^{-1}}$ determined by Knapp et al., the three K I velocity components have expansion velocities of -10.1, -11.0 and $-12.0\,\mathrm{km\,s^{-1}}$, consistent with all three components making a contribution to the CO emission, for which Knapp et al. measured an expansion velocity of $-10.7 \pm 1.1\,\mathrm{km\,s^{-1}}$. The mid-infrared dust emission images of Meixner et al. (1997) and Dayal et al. (1998) showed a morphology that was modelled as a result of a spherical outer shell containing an equatorially enhanced inner envelope. It is possible that these stuctures give rise to the the two main velocity components seen in our C_2 and K I absorption spectra. Multiple shells around post-AGB objects are not unprecedented, as evidenced by the *Hubble Space Telescope* optical imaging of many discrete circular arcs in the reflection nebulosity around the carbon-rich post-AGB object GL 2688 (Sahai et al. 1998).

All three circumstellar K I lines are extremely narrow, with *b*-values in the range 0.2–$0.3\,\mathrm{km\,s^{-1}}$. A velocity dispersion of $b(K\,\mathrm{I}) = 0.2\,\mathrm{km\,s^{-1}}$ gives a rigorous upper-limit to the kinetic temperature of 94 K. There is evidence from the rotational

excitation of C_2 (see below, also Bakker & Lambert 1998b) that the kinetic temperature in the region of *molecular* absorption is significantly lower than this ($T_k \lesssim 20$ K), suggesting either that an additional line broadening mechanism is present, or that the kinetic temperature deduced from the C_2 measurements is not appropriate for the region of K I absorption. Assuming that any additional line broadening is owing to 'turbulence' in the absorbing region, the velocity dispersion parameter is given by the expression

$$b = \sqrt{\frac{2kT_k}{m} + 2v_t^2}, \quad (1)$$

where T_k is the kinetic temperature, v_t is the one-dimensional rms turbulent velocity along the line-of-sight, m is the mass of the element under consideration, and k is Boltzmann's constant. Equation (1) indicates that, for lines formed in the same region of space, the ratio $b(\mathrm{K\,I})/b(C_2)$ must lie between the values of 0.78 (for $v_t = 0$) and 1.0 (for the case where turbulence dominates). Since the observed value of this ratio for the most red-shifted component (the only one which is well-defined in both K I and C_2) is 0.37 ± 0.09 it appears that neutral K must exist in a colder and/or less turbulent region than that where the bulk of the C_2 exists. This may be consistent with a shell structure such as that suggested by Bakker et al. (1996) where the C_2 is produced primarily by the photo-destruction of more complicated molecules (notably C_2H_2, e.g. Cherchneff, Glassgold & Mamon 1993) near the inner and/or outer surfaces of the shell, while neutral K might be expected to exist in the more shielded interior, where the photoionization rate would be lower.

Finally, we note that we find no evidence for K I counterparts of the interstellar components identified by Bakker et al. (1996). Although the limits placed on the interstellar K I column density are not strong [$N(\mathrm{K\,I}) < 6 \times 10^{10}$ cm^{-2}], owing to our poor signal-to-noise ratio, the contrast with the strong circumstellar components is striking. This presumably reflects a much higher density, and therefore higher recombination rate, in the circumstellar material compared to that typically found for interstellar clouds.

3.2 C_2

Fig. 3 shows close-ups of the six circumstellar C_2 lines observed towards HD 56126. The spectra are clearly dominated by a strong C_2 velocity component at $v_{\mathrm{helio}} \approx 77.6$ km s^{-1}. However, the two strongest lines, Q(2) and Q(4), also show clear evidence for a weaker component blueshifted by approximately 1 km s^{-1}, and this component is also plausibly present in all the other lines except R(14). It is notable that this velocity separation is essentially identical to that of the two strongest K I components discussed above (Table 1), lending credibility to its identification as a real circumstellar component. We find no convincing evidence for a C_2 component corresponding to the third (weakest and most blueshifted) component identified in K I, although higher signal-to-noise ratio observations might reveal that one is present at this velocity also.

The primary interest of the present work is determination of the intrinsic linewidths of the circumstellar molecular lines. From the measurements presented in Table 1 we obtain weighted mean velocity dispersions of $b(C_2) = 0.54 \pm 0.03$ km s^{-1} for the main velocity component, and a slightly larger value of $b(C_2) = 0.60 \pm 0.05$ km s^{-1} for the weaker component. We note that a velocity dispersion of 0.54 km s^{-1} results in a rigorous upper limit to the kinetic temperature of 420 K. It is of interest to compare these direct measurement of the C_2 velocity dispersion with previous estimates of the intrinsic widths of circumstellar molecular lines in the HD 56126 shell. From a curve-of-growth analysis of spectrally unresolved CN lines, Bakker & Lambert (1998a) obtained $b(\mathrm{CN}) = 0.51 \pm 0.04$ km s^{-1}, which is very similar to the values obtained for each of the C_2 components identified here. In a subsequent paper, Bakker & Lambert (1998b) performed a similar curve-of-growth analysis of four of the C_2 Phillips bands, but noted that, as the lines from a given rotational level in all four bands were not well spaced in equivalent width, it was difficult to define the curve-of-growth accurately. Moreover, they found difficulty in fitting the C_2 lines from different bands onto the same curve-of-growth without either (a) making arbitary adjustments to the theoretical band oscillator strengths or (b) adopting the very low velocity dispersion of $b(C_2) = 0.31 \pm 0.05$ km s^{-1}. As this low value is inconsistent with their more reliable determination of the CN velocity dispersion, Bakker & Lambert (1998b) chose to adopt the latter value (0.51 ± 0.04 km s^{-1}) for their determination of the C_2 column densities.

Our direct measurement of the C_2 linewidth ($b(C_2) = 0.54 \pm 0.03$ km s^{-1}) certainly excludes a value as low as 0.31 km s^{-1}, and to that extent vindicates Bakker & Lambert's (1998b) adoption of the larger CN value. We note, however, that our discovery of two closely spaced C_2 velocity components implies that a somewhat larger *effective* b-value would be appropriate for use with the combined equivalent widths obtained at lower resolution. For example, the measurements presented here for the Q(4) line (Table 1) imply an effective b value close to 0.75 km s^{-1} for the case where the two velocity components are not resolved. The fact that Bakker & Lambert (1998b) obtained a smaller b-value from the CN curve-of-growth may imply that the velocity structure in the two species is different, and perhaps that the weaker C_2 component does not have a counterpart in CN. This would would presumably reflect different physical and chemical conditions within the two C_2-bearing shells; only ultra-high-resolution observations of the CN lines themselves will be able to resolve this issue.

We note that the influence of unresolved velocity structure on the curve-of-growth can make a significant difference in the derived column densities for the stronger lines. For example, consider the Q(4) line, for which Bakker (1995) and Bakker et al. (1996) obtained an equivalent width of 50.0 mÅ (in close agreement with our value of 47 ± 1.4 mÅ). Adopting $b = 0.51$ km s^{-1}, this yields $N(J=4) = 4.96 \times 10^{14}$ cm^{-2}, which indeed agrees closely with the value of 4.68×10^{14} cm^{-2} given by Bakker & Lambert (1998b) on the basis of an average of six lines arising from this level. However, adoption of an *effective* b value of 0.75 km s^{-1} results in a column density of $N(J=4) = 1.98 \times 10^{14}$ cm^{-2}, a factor of 2.5 lower (and in good agreement with the *total* $J = 4$ column density of 1.73×10^{14} cm^{-2} given in Table 1). Thus, while our results support the C_2 velocity dispersion adopted by Bakker & Lambert (1998b), they also suggest that neglect of unresolved velocity structure has led them to overestimate the total C_2 column density.

In principle, studies of the rotational excitation of C_2 can be used to determine the temperature and density of interstellar and circumstellar material. It has long been known that the ground state rotational levels of the C_2 molecule in such environments are not in thermal equlibrium, owing to the competing effects of collisional excitation/de-excitation and radiative fluorescence and cascade (e.g. van Dishoeck 1984; van Dishoeck & Black 1982).

For this reason, no single excitation temperature can describe the rotational populations. The excitation temperature deduced from the lower-lying levels is expected to be a better approximation to the actual gas kinetic temperature, but is likely still to be an overestimate owing to the influence of radiative processes. In this respect we note that the $J = 2/J = 0$ excitation temperature deduced from the present observations is $T_{20} = 21$ K for the main C_2 velocity component. Allowing for the errors on the column densities, we obtain an upper limit of $T_{20} < 35$ K. As noted above, we expect the actual kinetic temperature to be somewhat lower.

Bakker & Lambert (1998b) have adopted van Dishoeck & Black's (1982) model of interstellar C_2 excitation in order to estimate the kinetic temperature, T_k, and density, n, of the circumstellar shell from the observed rotational excitation. In order to do this they have assumed that the circumstellar radiation field can approximated by a simple scaling of the *interstellar* radiation field. In so far as the photo-excitation of C_2 is mostly as a result of absorption of near infra-red photons in the A–X Phillips bands in the restricted wavelength range 0.8 and 1.2 μm (van Dishoeck & Black 1982; van Dishoeck 1984), this approach is probably valid. However, we note that it will overestimate the flux in the UV F–X and D–X bands, which also contribute to the radiative pumping of the molecule; clearly it would be desirable to develop models of C_2 excitation tailored to the specific radiation field of a circumstellar envelope.

In any case, adopting this procedure Bakker & Lambert (1998b) obtain $T_k = 25$ K and $n = 1.7 \times 10^7$ cm^{-3} for the region giving rise to the circumstellar C_2 absorption. We compare our results for the rotational excitation of the strongest C_2 component with those of Bakker & Lambert in Fig. 4. Our results are largely consistent with theirs because, although we obtain lower total column densities (for the reasons discussed above), the determination of physical conditions depends only on the *relative* column densities of the different rotational levels. Given the errors on the measurements, it is clear that there is no significant difference between these independent measurements.

Also shown in Fig. 4 are the theoretical populations predicted by the van Dishoeck & Black (1982) model, following the other assumptions made by Bakker & Lambert 1998b. Contrary to the temperature quoted by Bakker & Lambert ($T_k = 25$ K), we find that this model actually requires a significantly lower kinetic temperature ($T_k \approx 10$ K) in order to account for the $N(J = 2)/N(J = 0)$ column density ratio. Specifically, we find that $T_k = 25$ K results in $-\ln\{5N_0/N_2\} \approx -0.5$ (only weakly dependent on density), which is right at the upper limit of our errorbar for this value in Fig. 4, whereas $T_k = 10\,K$ yields a value of -0.88, much closer to the values actually measured both here and by Bakker & Lambert (1998b). Such a low value of T_k is consistent with measurements for other post-AGB objects; for example, in the O-rich Boomerang Nebula, Sahai & Nyman (1997) have detected CO in absorption against the microwave background (implying $T_k < 3$ K), which they interpreted as because of the effect of strong adiabatic cooling in the expanding outflow, combined with significant self-shielding against external heating sources.

The solid curve in Fig. 4 shows the theoretical populations (van Dishoeck 1984) for $T_k = 10$ K and $n_c\sigma_0/I = 3 \times 10^{-14}$ cm^{-1} (where n_c is the number density of C_2 collision partners, σ_0 is the C_2 collisional cross-section, and I is a scaling factor for the radiation field). This is essentially the same value found by Bakker & Lambert (1998b), and as noted by them implies $n_c = 1.6 \times 10^7$ cm^{-3} for $I = 4.1 \times 10^5$. We note, however, that this particular value of I has been obtained by assuming that the C_2 molecules lie at a distance of 1.1×10^{16} cm (2354 R_*) from the star (Bakker et al. 1997). Meixner et al. (1997) have recently obtained an inner radius for the *dust* shell of 4.5×10^{16} cm from a study of the infrared emission (although this distance is uncertain by a factor two, owing to the uncertainty in the stellar distance). If the C_2 molecules are located as far as this from the central star the radiation field will be over an order of magnitude lower, resulting

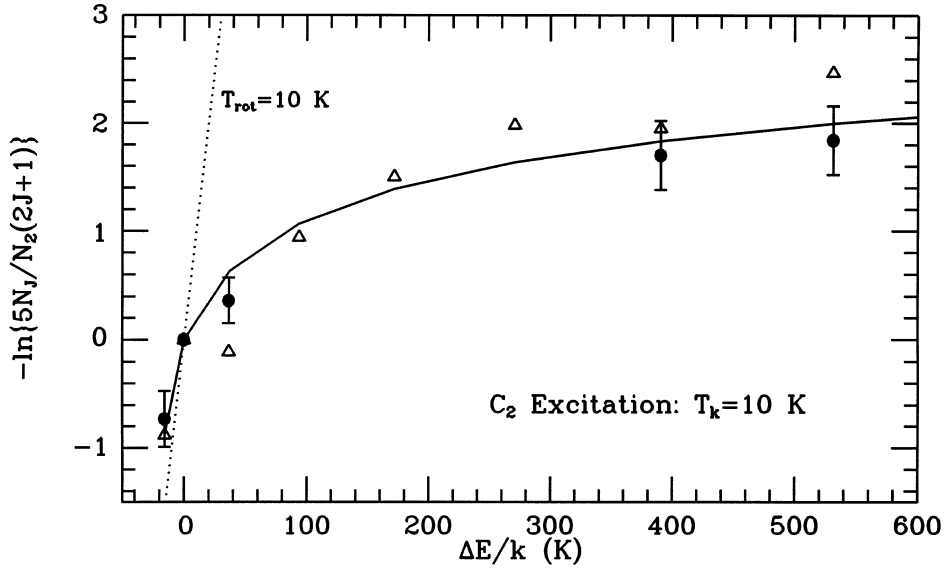

Figure 4. Relative rotational-level populations of C_2 with respect to $J = 2$, as a function of excitation potential, for the main circumstellar velocity component towards HD 56126. Solid circles with error bars indicate the results obtained here, while open triangles show those obtained by Bakker & Lambert (1998b). The solid curve gives the theoretical populations, taken from van Dishoeck (1984), for $T_k = 10$ K and $n_c\sigma_0/I = 3 \times 10^{-14}$ cm^{-1} (where σ_0 is the C_2 collisional cross-section, and I is a scaling factor for the radiation field). For $I = 4.1 \times 10^5$ and $\sigma_0 = 7.8 \times 10^{-16}$ cm^{-2} (following Bakker & Lambert 1998b) this corresponds to a shell density of 1.6×10^7 cm^{-3}, although the value of I depends sensitively on the assumed distance of the shell from the star (see text). The dotted line, labelled $T_{rot} = 10$ K, gives the equilibrium thermal populations at this temperature.

in $n_c \approx 10^6\,\mathrm{cm}^{-3}$. Clearly, measurement of the shell density by this method, and therefore any statements regarding the stellar mass-loss rate, depend critically on determining the thickness of the molecular shell and its distance from the star.

A kinetic temperature of $T_k \approx 10\,\mathrm{K}$ is much lower than the rigorous upper limit of $T_k < 420\,\mathrm{K}$ deduced from the linewidth measurements, and this implies that another line-broadening mechanism must be present. If this additional broadening is as a result of turbulence, equation (1) yields $v_t = 0.38\,\mathrm{km\,s}^{-1}$ for $b = 0.54\,\mathrm{km\,s}^{-1}$ and $T_k = 10\,\mathrm{K}$. The full three-dimensional turbulent velocity, $\sqrt{3}v_t$, is thus $0.66\,\mathrm{km\,s}^{-1}$. At a temperature of 10 K, the isothermal sound speed in a molecular hydrogen gas (with 10 per cent He by number) is $0.19\,\mathrm{km\,s}^{-1}$, so if turbulence is responsible for broadening the line profiles it would appear to be supersonic. This is less of a problem in a circumstellar, as opposed to an interstellar, environment as a local energy source to drive the turbulence is available. However, it is also possible that the lines might be broadened by a velocity *gradient* through the absorbing region(s). In principle, this might be detectable by an asymmetry in the observed line profiles, although the present data lack the signal-to-noise ratio necessary to identify such an effect.

4 CONCLUSIONS

We have obtained observations of circumstellar K I and C_2 towards the post-AGB star HD 56126. The very high spectral resolution of these observations ($0.35\,\mathrm{km\,s}^{-1}$ FWHM) has enabled us to resolve fully the intrinsic line profiles for the first time, and thereby place new limits on the physical conditions prevailing in the circumstellar material. Our principal results are as follows.

(i) We find clear evidence for multiple velocity structure within the circumstellar environment, with three discrete velocity components present in K I and two in C_2. We suggest that this velocity structure is because of several distinct circumstellar shells around HD 56126, indicative of episodic mass-loss events during its late AGB and post-AGB evolution.

(ii) The individual circumstellar velocity components are all extremely narrow. The three K I components have *b*-values in the range 0.2–$0.3\,\mathrm{km\,s}^{-1}$, which correspond to rigorous kinetic temperature upper limits, T_k^{ul} in the range 94–211 K. The strongest (and therefore best defined) C_2 component has a *b*-value (determined from a weighted average of six lines) of $0.54 \pm 0.03\,\mathrm{km\,s}^{-1}$, essentially identical to the value of $0.51 \pm 0.04\,\mathrm{km\,s}^{-1}$ obtained by indirect means for circumstellar CN towards this object (Bakker & Lambert 1998a). This yields an upper limit to the temperature of $T_k^{ul} = 420\,\mathrm{K}$. Assuming a kinetic temperature of $T_k = 10\,\mathrm{K}$ from the C_2 rotational excitation, this implies a three-dimensional turbulent velocity of $\sqrt{3}v_t = 0.66\,\mathrm{km\,s}^{-1}$, which is certainly supersonic given that the isothermal sound speed at this temperature is $0.19\,\mathrm{km\,s}^{-1}$.

(iii) We find that the observed velocity dispersion ratio, $b(\mathrm{K\,I})/b(C_2) = 0.37 \pm 0.09$, is inconsistent with the K I and C_2 lines being formed under the same physical conditions, in spite of the velocity agreement between them. This indicates that K I arises primarily in a colder and/or less turbulent region of the shell than the C_2, probably in a shielded interior where the photo-ionization rate is lower.

(iv) We obtain significantly lower C_2 column densities than Bakker & Lambert (1998b), even though our equivalent widths are comparable (Table 1), apparently owing to the influence of unresolved velocity structure on their study. Within the limits imposed by the measuring errors, we obtain a similar result for the rotational excitation of the molecule (Fig. 4), although we argue that this implies a kinetic temperature of $T_k \approx 10\,\mathrm{K}$ rather than their adopted value of 25 K. We concur with Bakker & Lambert's derivation of a shell density of $n \approx 1.6 \times 10^7\,\mathrm{cm}^{-3}$ (given their other assumptions), but note that this depends on the general applicability of the *interstellar* C_2 excitation model of van Dishoeck & Black (1982). Clearly it would be desirable to develop models of C_2 excitation tailored to the specific conditions of a circumstellar envelope.

ACKNOWLEDGMENTS

We thank PATT for the award of telescope time. We are grateful to Professor Ewine van Dishoeck for helpful correspondence concerning the excitation of C_2, and to the referee (Professor S.R. Federman) for helpful and detailed comments on the original version of this paper. IAC thanks PPARC for the award an Advanced Fellowship.

REFERENCES

Barlow M. J., Crawford I. A., Diego F., Dryburgh M., Fish A. C., Howarth I. D., Spyromilio J., Walker D. D., 1995, MNRAS, 272, 333
Bakker E. J., 1995, PhD thesis, Univ. Utrecht
Bakker E. J., Lambert D. L., 1998a, ApJ, 502, 417
Bakker E. J., Lambert D. L., 1998b, ApJ, 508, 387
Bakker E. J., Waters L. B. F. M., Lamers H. J. G. L. M., Trams N. R., Van der Wolf F. L. A., 1996, A&A, 310, 893
Bakker E. J., van Dishoeck E. F., Waters L. B. F. M., Schoenmaker T., 1997, A&A, 323, 469
Cherchneff I., Glassgold A. E., Mamon G. A., 1993, ApJ, 410, 188
Dayal A., Hoffman W. F., Bieging J. H., Hora J. L., Deutsch L. K., Fazio G. G., 1998, ApJ, 492, 603
Diego F., 1993, Appl. Opt., 32, 6284
Diego F. et al., 1995, MNRAS, 272, 323
Gustafsson B., Eriksson K., Kiselman D., Olander N., Olofsson H., 1997, A&A, 318, 535
Hrivnak B. J., Kwok S., 1991, ApJ, 371, 631
Hrivnak B. J., 1995, ApJ, 438, 341
Howarth I. D., Murray J., Mills D., 1993, Starlink User Note, No. 50
Knapp G. R., Young K., Lee E., Jorissen A., 1998, ApJS, 117, 209
Kwok S., Volk K. M., Hrivnak B. J., 1989, ApJ, 345, L51
Kwok S., Hrivnak B. J., Geballe T. R., 1995, ApJ, 454, 394
Mauron N., Querci F., 1990, A&AS, 86, 513
Meixner M., Skinner C. J., Graham J. R., Keto E., Jernigan J. G., Arens J. F., 1997, ApJ, 482, 897
Morton D. C., 1991, ApJS, 77, 119
Sahai R., Nyman L.-A., 1997, ApJ, 487, L155
Sahai R. et al., 1998, ApJ, 493, 301
Shortridge K., 1988, Starlink User Note, No. 86
van Dishoeck E. F., 1984, PhD thesis, Univ. Leiden
van Dishoeck E. F., Black J. H., 1982, ApJ, 258, 533
Welty D. E., Hobbs L. M., Kulkarni V. P., 1994, ApJ, 436, 152

This paper has been typeset from a TEX/LATEX file prepared by the author.